ELSEVIER

Journal of Power Sources 112 (2002) 649–654

JOURNAL OF POWER SOURCES

www.elsevier.com/locate/jpowsour

Short communication

Graphite–FeSi alloy composites as anode materials for rechargeable lithium batteries

Heon-Young Lee, Sung-Man Lee*

Department of Advanced Materials Science and Engineering, Kangwon National University, Chuncheon, Kangwon-Do 200-701, South Korea

Received 30 May 2002; accepted 17 August 2002

Abstract

Iron–silicon are prepared by annealing elemental mixtures at 1000 °C followed by mechanical milling. Graphite–$Fe_{20}Si_{80}$ alloy composites have been prepared by ball-milling a mixture of $Fe_{20}Si_{80}$ alloy and graphite powder. The microstructure and electrochemical performance of the composites are characterized by X-ray diffraction and an electrochemical method. The $FeSi_2$ matrix is stable for extended cycles and acts as a buffer for the active centre, Si. The $Fe_{20}Si_{80}$ alloy electrode delivers large initial capacity, but the capacity degrades rapidly with cycling. $Fe_{20}Si_{80}$ alloy–graphite composite electrodes, however, show good cycleability and a high reversible capacity of about 600 mAh g^{-1}. These composites appear to be promising candidates for negative electrodes in lithium rechargeable batteries.

Keywords: Rechargeable lithium batteries; Fe–Si alloy; Composite electrode; Negative electrode; Ball-milling

1. Introduction

Much attention has focused on improving the specific capacity of the anode material in rechargeable lithium batteries. Graphitic carbons are commonly used as anodes in most commercial cells.

Their storage capacities, however, are limited to 372 mAh g^{-1}. Several materials, especially tin-based oxides, have recently been reported as possible anode materials to replace the carbon system [1–3]. Despite the interesting performance of these materials, a large irreversible loss in capacity is a main limitation to their use as anode materials in lithium rechargeable batteries. It is well known that silicon can also react with lithium to form Li_xSi alloys with a maximum capacity of up to 4000 mAh g^{-1} [4,5]. Nevertheless, the alloying process does not appear to be sufficiently reversible due to large volume changes during cycling which lead to pulverization of the silicon powders [6]. Recently, it has been reported [7,8] that metal silicide alloys can be as an anode material for lithium rechargeable batteries.

In this investigation, the preparation and electrochemical performance of $Fe_{27}Si_{73}$, $Fe_{20}Si_{80}$ and graphite–$Fe_{20}Si_{80}$ alloy composites is reported. The graphite–$Fe_{20}Si_{80}$ alloy composite electrodes demonstrate quite a high reversible capacity with excellent cycleability.

2. Experimental

Iron–silicon alloy powders were prepared by annealing an elemental mixture at 1000 °C for 2 h under a flow of argon, followed by milling with a high-energy ball-mill (SPEX mixer/mill 8000). A stainless-steel vial and stainless-steel balls of 7.9 mm in diameter were used for milling. The ratio of ball mass to mixture load was 10:1. The alloy powders were characterized by X-ray diffraction (XRD) analysis using Cu Kα radiation. 50:50 (wt.%) mixtures of the pure graphite (Timrex SFG6) and Fe–Si alloy powders were prepared by ball-milling in a planetary mill (pulverisette-7, Fritsch) for 0.5–2 h at a rotation rate of 1600 rpm in an argon atmosphere.

Coin cells (type 2016) were fabricated to test the electrochemical properties. The ball-milled Fe–Si alloy powders were mixed with 15 wt.% acetylene black (AB) as an electron conductor and 10 wt.% poly-(vinylidene fluoride) (PVDF) solution dissolved in *N*-methyl-2-pyrrolidone (NMP) as a binder. The graphite–$Fe_{20}Si_{80}$ alloy composite electrodes were made by dispersing 90 wt.% active materials and 10 wt.% PVDF binder in NMP solvent. The resultant slurries were spread on a copper mesh, dried at 120 °C under vacuum overnight to remove the NMP, and then pressed into a sheet. The electrolyte was 1 M $LiPF_6$ in a mixture of ethylene carbonate (EC) and diethyl carbonate (DEC) (1:1 by volume, provided by Cheil Industries Inc., South Korea). Half-cells were assembled in an argon-filled glove-box. The

* Corresponding author. Tel.: +82-33-250-6266; fax: +82-33-242-6256.
E-mail address: smlee@kangwon.ac.kr (S.-M. Lee).

0378-7753/02/$ – see front matter
PII: S0378-7753(02)00461-5

cells were galvanostatically charged and discharged in the voltage range 0–2 V versus Li/Li^+.

3. Results and discussion

The XRD patterns of $Fe_{27}Si_{73}$ alloy powders after annealing at 1000 °C and ball-milling are presented in Fig. 1. The pattern of the annealed sample was indexed with the reflections of α,β-$FeSi_2$ and silicon. After ball-milling, the reflection lines of disappear and only the α,β-$FeSi_2$ phase is detected. The peaks broaden with milling time and the intensities drastically decrease. Line-broadening is due to grain refinement and lattice internal strain.

The discharge capacity of the ball-milled $Fe_{27}Si_{73}$ with cycle number is presented in Fig. 2, in which the data for $FeSi_2$($Fe_{33.3}Si_{66.7}$) is also indeed for the purpose of comparison. It appears that the discharge capacity of the $Fe_{27}Si_{73}$ electrode appears to be due to the nano-dispersed silicon $FeSi_2$ matrix. The $FeSi_2$ phase is stable during cycling and

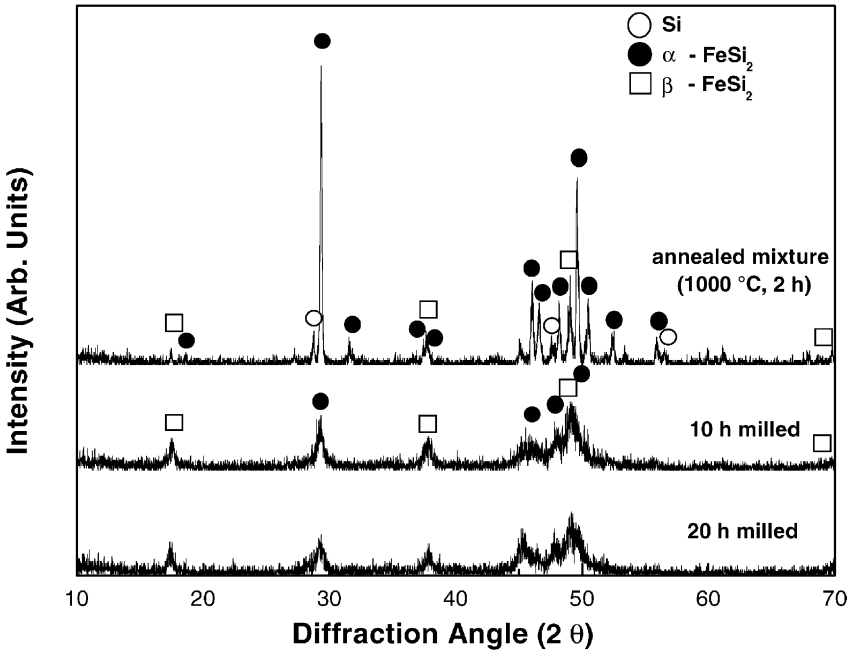

Fig. 1. XRD patterns of $Fe_{27}Si_{73}$ alloy after annealing at 1000 °C for 2 h and ball-milling.

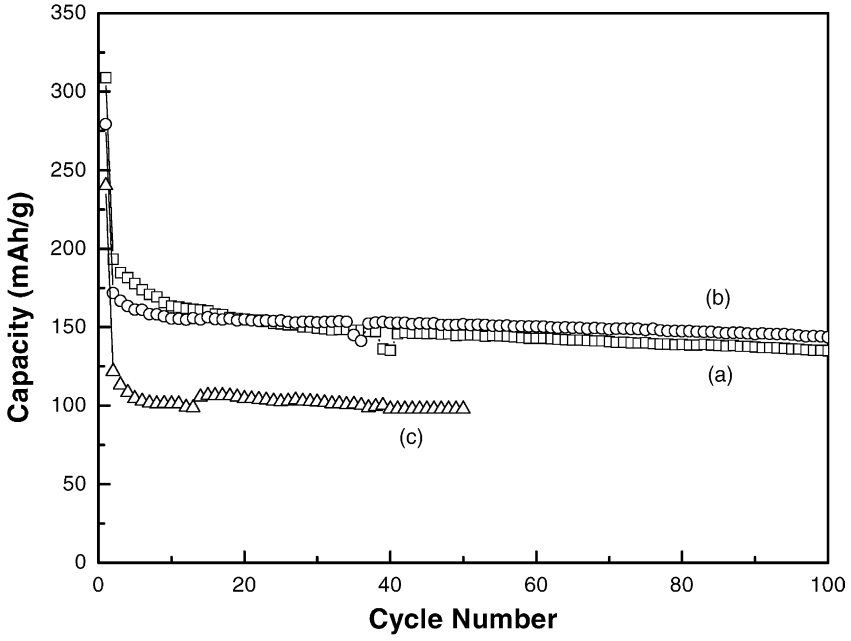

Fig. 2. Discharge capacity vs. cycle number for $Fe_{27}Si_{73}$ alloy ball-milled for (a) 10 h, (b) 20 h, and $FeSi_2$ ($Fe_{33.3}Si_{66.7}$) alloy electrodes.

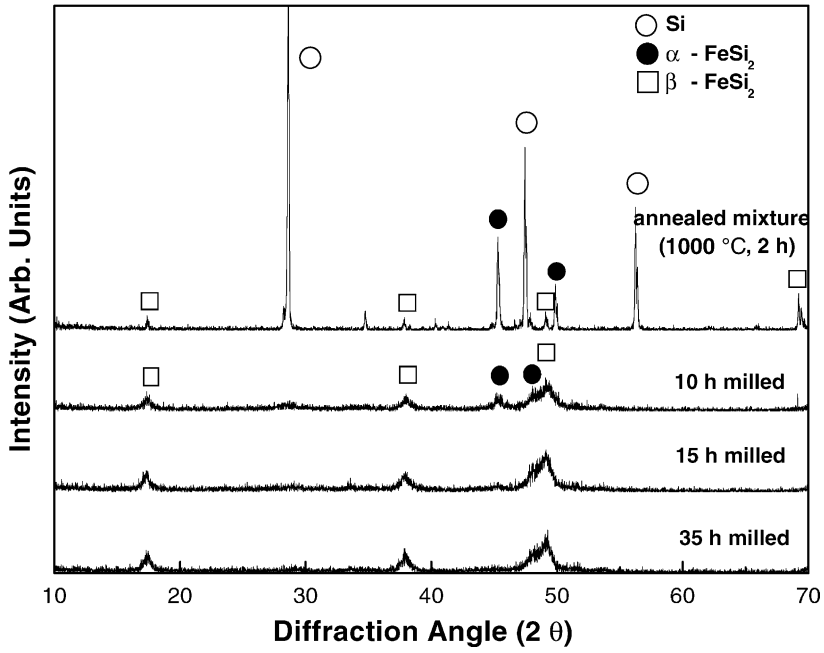

Fig. 3. XRD patterns of $Fe_{20}Si_{80}$ alloy after annealing and ball-milling.

acts as a buffering matrix for the formation of Li_xSi during cycling. As a result, the capacity is very stable with cycling.

A study has been made of the electrochemical performance of an $Fe_{20}Si_{80}$ alloy which contains a large amount of silicon as the active centre. The effect of mechanical milling on the annealed $Fe_{20}Si_{80}$ alloy shown in Fig. 3 in the form of XRD patterns. With ball-milling, the silicon peaks vanished and the α,β-$FeSi_2$ peaks broaden. This behaviour is similar to that observed for $Fe_{27}Si_{73}$ in Fig. 1. The discharge capacity of ball-milled $Fe_{20}Si_{80}$ alloys is plotted as a function of cycle number in Fig. 4. Ball-milled $Fe_{20}Si_{80}$ alloys deliver a large initial lithium insertion capacity, but the capacity degrades with cycling quite rapidly. This is probably because there is insufficient $FeSi_2$, phase to buffer the expansion of the silicon domain during lithium insertion, as inferred from Figs. 1 and 2. This problem can be solved by incorporating ductile graphite to act as a buffer for the active centre.

Discharge capacity as a function of cycle number for ball-milled graphite–$Fe_{20}Si_{80}$ alloy composite electrodes is

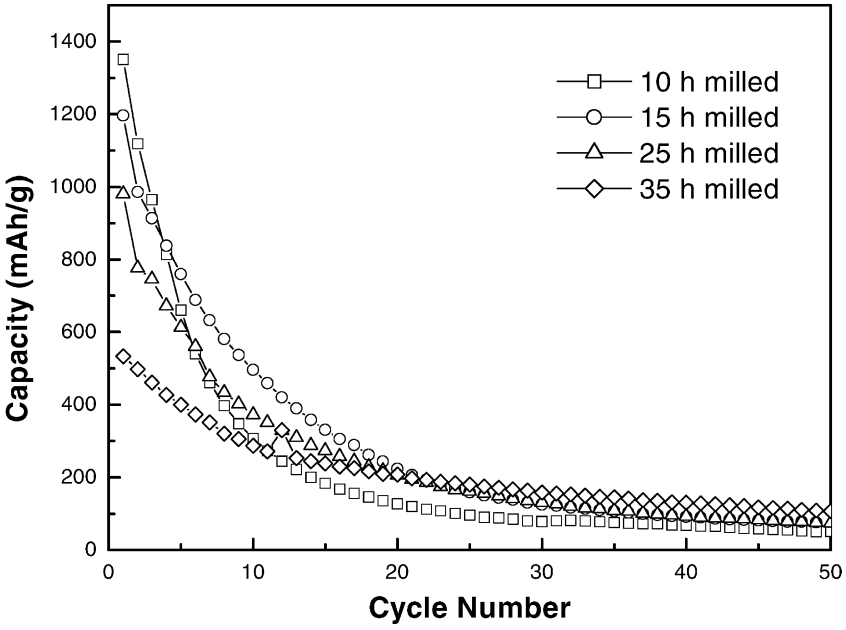

Fig. 4. Discharge capacity vs. cycle number for ball-milled $Fe_{20}Si_{80}$ alloys.

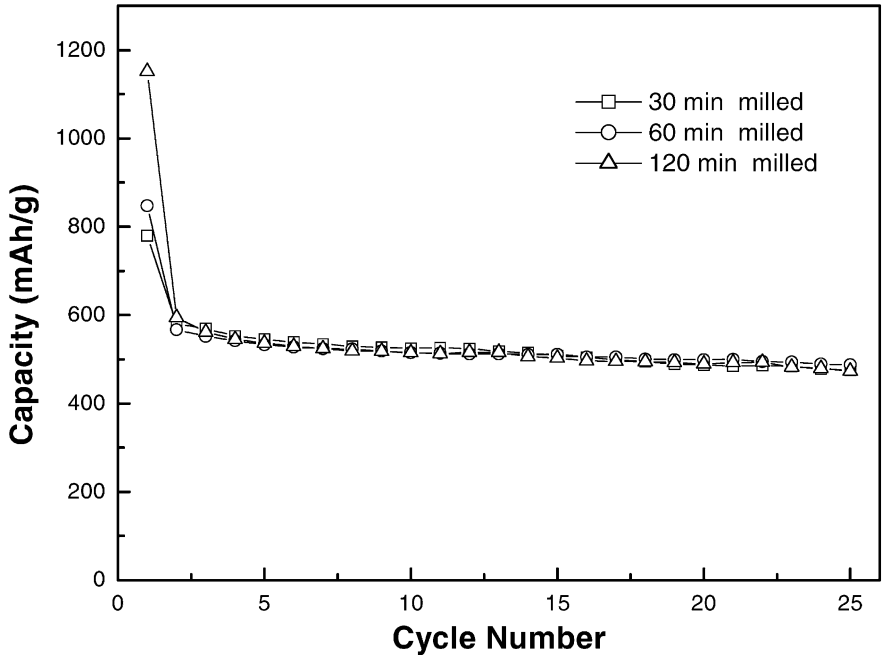

Fig. 5. Discharge capacity vs. cycle number for ball-milled graphite–$Fe_{20}Si_{80}$ alloy composite electrodes. $Fe_{20}Si_{80}$ alloy was pre-milled for 15 h. The cells were cycled between 0.0 and 2 V.

presented in Fig. 5. As expected, the cycleability of the composite electrodes have been significantly improved. A reversible capacity of ~600 mAh g^{-1} is obtained. It appears that ball-milling of a mixture of graphite and $Fe_{20}Si_{80}$ alloy powders leads to an increase in irreversible capacity the first charge–discharge. This irreversible capacity, mainly between 0.9 and 0.7 V, is supposed to be caused by electrolyte decomposition and the formation of a passivation film on the carbon particles [9,10], as shown in Fig. 6. The XRD patterns of ball-milled graphite–$Fe_{20}Si_{80}$ alloy composites are shown in Fig. 7. For comparison, the XRD pattern of the unmilled graphite is also shown. After ball-milling, the diffraction peaks of graphite become very broad and the peak intensity decreases due to the reduction of particle size

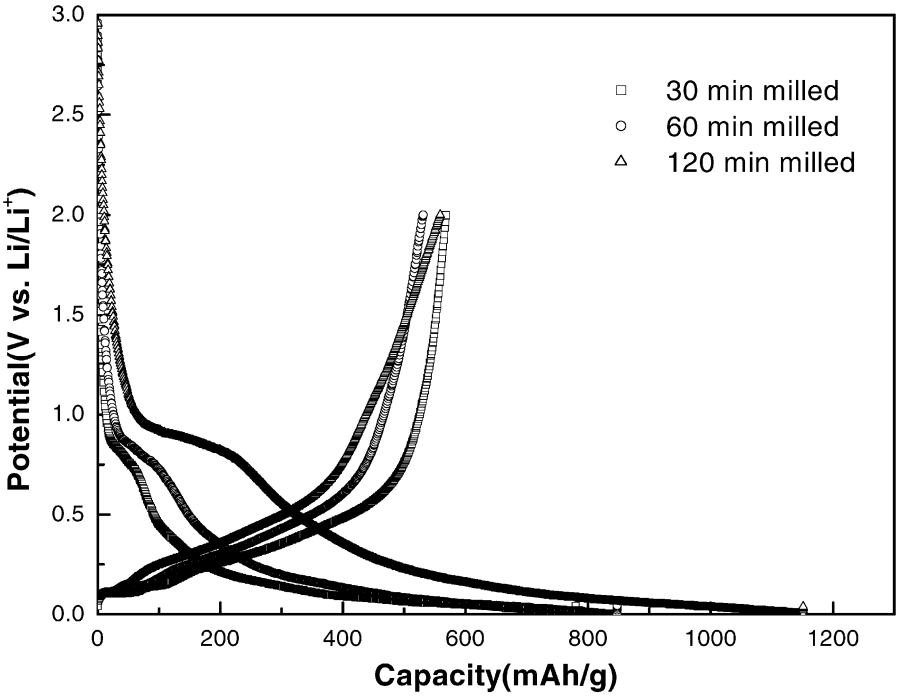

Fig. 6. First discharge and charge curves of ball-milled graphite–$Fe_{20}Si_{80}$ alloy composite electrodes.

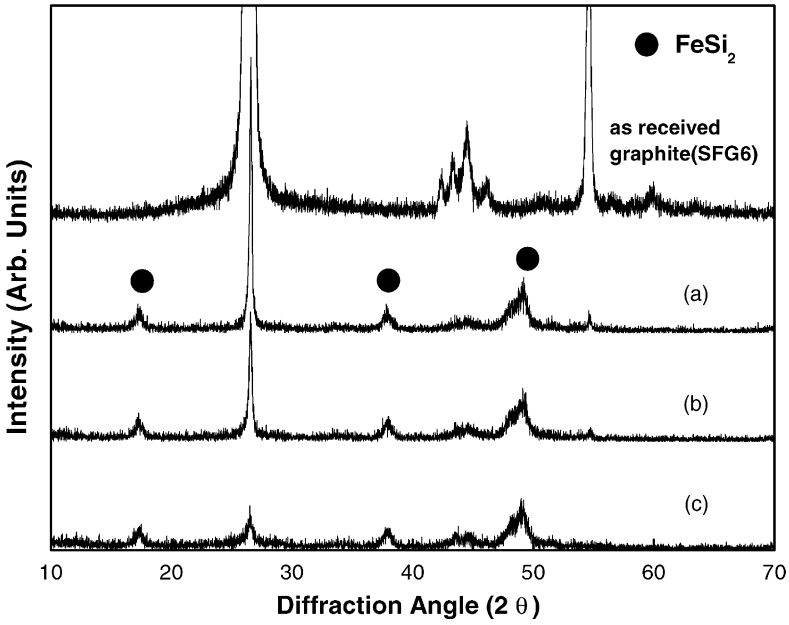

Fig. 7. XRD patterns of ball-milled graphite–$Fe_{20}Si_{80}$ alloy composites after (a) 30 min milling, (b) 60 min milling, (c) 120 min milling.

and disordering, while the diffraction peaks for Fe–Si alloy remain unchanged. Nevertheless, it is noted that the effect of ball-milling on the cycleability and the reversible capacity of the composite electrodes is negligible. It is well known that the cycling performance can be improved by restricting the voltage range for cycling [11,12]. The discharge capacity versus cycle number for the composite electrode cycled between 0.0 and 1.2 V is given in Fig. 8. When the upper cut-off voltage is reduced to 1.2 V, better cycling behaviour is obtained. The coulombic efficiencies of $Fe_{20}Si_{80}$ alloy and composite electrodes as a function of cycle number are presented in Fig. 9. The cycling efficiency of composite electrode is about 99% after five cycles, which is superior to that of the $Fe_{20}Si_{80}$ alloy electrode. It is though that the electrode performance can be further improved by optimizing the ball-milling conditions to produce $Fe_{20}Si_{80}$ alloy with appropriate microstructure and composite powders. These preliminary results suggest that graphite–$Fe_{20}Si_{80}$

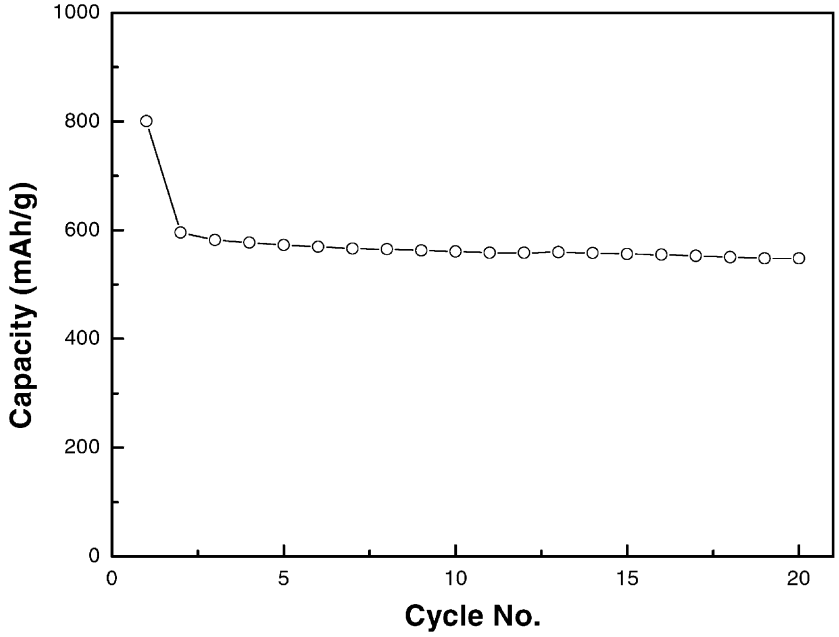

Fig. 8. Discharge capacity vs. cycle number for graphite–$Fe_{20}Si_{80}$ al1oy composite electrode (the 30 min ball-milled composite sample from Fig. 6). The cell was cycled between 0.0 and 1.2 V.

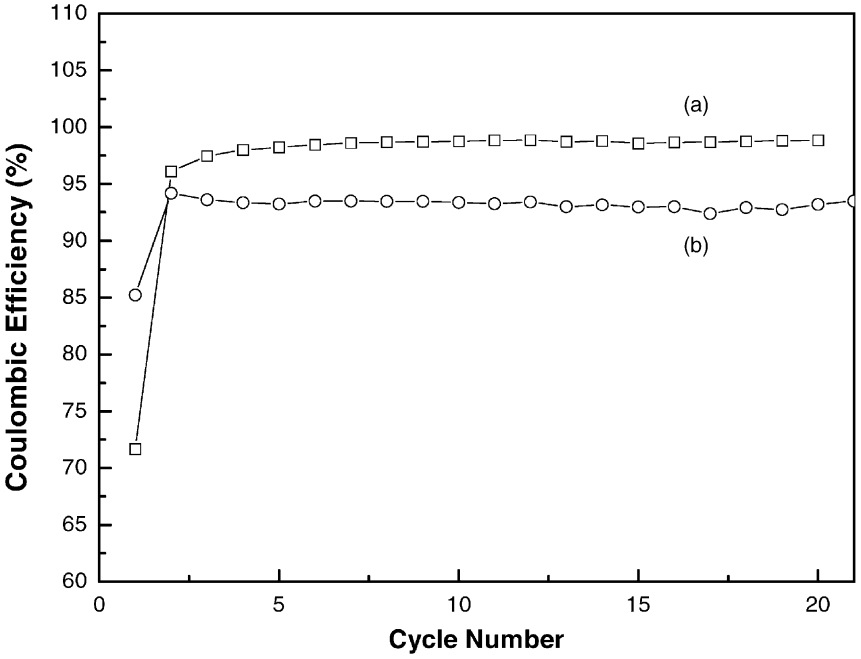

Fig. 9. The coulombic efficiencies of $Fe_{20}Si_{80}$ alloy and composite electrodes as a function of cycle number (a) 30 min ball-milled graphite–$Fe_{20}Si_{80}$ alloy composite electrode, (b) $Fe_{20}Si_{80}$ alloy electrode.

alloy composite is a promising alternative to carbons as a negative electrode material in rechargeable lithium batteries.

4. Conclusions

In this study, Fe–Si alloys and graphite–$Fe_{20}Si_{80}$ alloy composite are investigated as possible negative electrode materials for rechargeable lithium batteries. For an Fe–Si alloy, like $Fe_{27}Si_{73}$, which is slightly rich in the silicon, the $FeSi_2$ phase can act as a buffering matrix for the active centre, Si, during cycling. This leads to good cycling stability. An $Fe_{20}Si_{80}$ alloy with a large excess of silicon shows a decrease in capacity with cycle number. On the other hand, the $Fe_{20}Si_{80}$ alloy–graphite composite electrode, obtained by mechanical mixing with graphite, shows a good cycleability and a high reversible capacity of ~600 mAh g^{-1}, which suggests that an $Fe_{20}Si_{80}$ alloy–graphite composite is a prospective anode material for lithium rechargeable batteries.

Acknowledgements

This work was supported by the Ministry of Information & Communication of Korea (“Support project of University Information Technology Research Center” supervised by KIPA). The research was also supported, in part, by KISTEP through NRL Projects.

References

[1] V. Idota, T. Kubota, A. Matsufuji, Y. Maekawa, T. Miyasaka, Science 276 (1997) 1395.
[2] I.A. Courtney, J.R. Dahn, J. Electrochem. Soc. 144 (1997) 2045.
[3] I.A. Courtney, W.R. Mckinnon, J.R. Danh, J. Electrochem. Soc. 146 (1999) 59.
[4] R.A. Sharma, R.N. Seefurth, J. Electrochem. Soc. 123 (1976) 1763.
[5] B.A. Boukamp, G.C. Lesh, R.A. Huggins, J. Electrochem. Soc. 128 (1981) 725.
[6] K. Li, X. Huang, L. Chen, Z. Wu, Y. Liang, Electrochem. Solid State Lett. 2 (1999) 547.
[7] w. J Weydanz, M. Wohlfahrt-Mehrens, R.A. Huggins, J. Power Sources 81/82 (1999) 237.
[8] G.X. Wang, L. Sun, D.H. Bradhurst, S. Zhong, S.X. Dou, H.K. Liu, J. Power Sources 88 (2000) 278.
[9] R. Fong, U. Von Sacken, J.R. Dahn, J. Electrochem. Soc. 137 (1990) 2009.
[10] M. Winte, P. Novak, A. Monnier, J. Electrochem. Soc. 145 (1998) 428.
[11] O. Mao, R.A. Dunlap, J.R. Dahn, J. Electrochem. Soc. 146 (1999) 405.
[12] K.D. Kepler, J.T. Vaughey, M. Thackeray, Electrochem. Solid State Lett. 2 (1999) 307.